



Transactions of the Canadian Society for Mechanical Engineering

Failure phenomena in metallic and metal-lined polymer composite pressure vessels for aerospace applications

Journal:	<i>Transactions of the Canadian Society for Mechanical Engineering</i>
Manuscript ID	TCSME-2020-0204.R1
Manuscript Type:	Article
Date Submitted by the Author:	27-Nov-2020
Complete List of Authors:	C P, Goldin Priscilla; Universal College of Engineering and Technology, J, Selwin Rajadurai; Alagappa Chettiar Government College of Engineering and Technology
Keywords:	Metal-lined, Polymer composite, Pressure vessels, Burst pressure, aerospace
Is the invited manuscript for consideration in a Special Issue? :	Not applicable (regular submission)

SCHOLARONE™
Manuscripts

Failure phenomena in metallic and metal-lined polymer composite pressure vessels for aerospace applications

Goldin Priscilla C P^{1*} and Selwin Rajadurai J²

Faculty of Mechanical Engineering

¹ *Universal College of Engineering & Technology, Vallioor - 627 117, India*

² *Alagappa Chettiar Government College of Engineering & Technology,
Karaikudi-630004, India*

*Corresponding author: email-christogoldin@gmail.com

Draft

Abstract

Metallic and metal-lined polymer composite pressure vessels are extensively used in industries including aerospace. In the absence of unique failure criteria for the structural elements, phenomenological or empirical methodologies always fascinate the researchers. This paper deals with comprehensive methodologies in the prediction of burst pressure of metallic and metal-lined polymer composite pressure vessels for aerospace applications. Metallic pressure vessels are analyzed using Ansys software considering the elastic-plastic nature of materials. The progressive analysis is carried out in metal-lined composite pressure vessels in an explicit mode using Ansys software. The problem of solution convergence is discussed in detail. The extent of degradation in static analysis is suggested after multiple analysis trials. In the unit pressure extrapolation technique, stress components are evaluated using Ansys software, transformed into the local coordinate system and hence failure pressure of the first ply is identified by maximum stress criterion. Then the analysis is continued with degrading of failed layers using Ansys software and successive failures of layers are identified in steps. The results of burst pressure, evaluated through the present analyses show good agreement with the published test results. The procedures described in the paper would be of interest to the designers of pressure vessels.

Keywords: Metal-lined, Polymer composite, Pressure vessels, aerospace, Burst pressure.

1. Introduction

Metallic and metal-lined polymer composite pressure vessels find valuable applications in various fields of engineering as also in aerospace. Understanding the phenomenon of failure concerning the material behaviour and micromechanics is interesting to the designers. Undoubtedly experimentation is essential in the venture, but it is not always amenable to a single agency due to the involvement of high cost and time. In this context simulation of mechanical behaviour of materials and structures help the designers to a great extent. Finite element analysis has been proven to be a dependable tool for simulation of elastic and inelastic behaviour of materials. This paper attempts to demonstrate simple methodologies with the help of finite element analysis software Ansys for the burst pressure prediction of metallic and metal-lined polymer composite pressure vessels. Failure data from published literature has been utilized for verification of the accuracy of the procedures.

With regard to the metallic pressure vessels, one of the early researches is found in the work of Svensson (1958) wherein failure pressure of cylindrical and spherical pressure vessels made of strain hardening metals have been estimated. The materials were to have stress-strain relationship of Ludwik power law. He derived a pressure – deformation equation, assuming octahedral shear values for effective stress and strain. He used a failure criterion in which, the failure occurs at an additional strain when the pressure begins to decrease. Wei (1965), Margetson (1978), and Beena et al. (1995) have carried out experimental and analytical studies in the failure-predictions of rocket motor cases. Followed by many such authors contributing to this field, Christopher et al. (2002) made a comparative study on failure pressure estimations of unflawed cylindrical pressure vessels. Kadam et al. (2018) have conducted studies with finite element analysis considering limits of effective strain. Here, it is intended to demonstrate alternative analytical and finite element analysis

procedures in the light of the above literature for the failure pressure prediction of metallic rocket motor cases.

Owing to the major concern of structural efficiency in the aerospace industry, metal-lined composite pressure vessels have been developed. Metal-lining is used in polymer composite pressure vessels for both load sharing and prevention of leak (Sorrentino and Tersigni 2015). Kam et al. (1997) and Chang (2000) provide a good account of composite pressure vessel failure by first ply failure mode. Final failure or burst pressure is much higher than the first ply failure pressure. Though first ply failure pressure is sufficient for the preliminary design of composite pressure vessels, knowledge of burst pressure is essential in order to assess the factor of safety under the given loading.

Many researchers (Hu et al. 2009, Kalaycioglu and Dirikolu 2010, Wolford and Hyer (2005), Xu et al. 2009 and Liu et al. 2014) have conducted experimental as well as progressive failure approaches using finite element analysis software in the prediction of burst pressure of metal-lined polymer composite pressure vessels. They have used various failure criteria such as maximum stress criterion, Hashin criterion, Tsai – Hill, and Tsai – Wu. Rafiee et al. (2018) have employed both continuum damage mechanics (CDM) and ply discount method while evaluating theoretical burst pressure of filament wound composite tubes under internal pressure by progressive failure analysis. Rafiee and Elasmı (2017) have successfully predicted the fatigue life of composite pressure vessels using Cumulative fatigue damage modelling (CFDM). This technique is similar to CDM in progressive modelling, but with the knowledge of fatigue life curves of the composite material. Sleight (1999) describes progressive failure analysis methodology for laminated composite structures and recommends the use of non – interactive criterion such as maximum stress theory since they provide the failure mode. Accordingly, the maximum stress criterion is followed in this study. In the progressive failure analysis, due to the solution convergence difficulties arising from

the degradation of elastic properties, they have used a damage model, which is complex. They have made negative remarks on the results obtained while using the damage model. Wu et al. (2015) have conducted progressive failure analysis using maximum stress criterion and maximum strain criterion, with and without the use of a damage evolution model. They also have commented on the approach using the damage evolution model to be less accurate. In the absence of damage evolution models, material property degradation poses problems of non-convergence of solution (Wu et al. 2015). Textbook (Kaw 2015) gives a recommendation that the matrix failed ply can be replaced with a degraded one that has near-zero stiffness and strength in transverse and shear directions. The ply is to be fully discounted only when the fibre also fails. He has left the philosophy of assigning the extent of degradation to the user. Martins et al. (2014) and Bai et al. (2019) recommend a multiplication factor of 10^{-1} and 10^{-6} respectively for stiffness degradation. In this work, multiple trials and studies have been carried out and arrived at an extent of degradation for successful analysis.

2. Analysis of metallic cylinders

The pressure-deformation relationship derived by Svensson assumes the material behaviour as per Ludwik power law given by,

$$\sigma = \sigma_0 \varepsilon^n \quad (1)$$

Where σ and ε are true stress and true strain respectively. n is strain hardening exponent and σ_0 is material constant with the unit of stress.

Equation for burst pressure of thin cylinder by Svensson (1958) is,

$$p_b = \frac{2}{(\sqrt{3})^{n+1}} \sigma_{ult} \frac{t}{R_i} \quad (2)$$

Where, σ_{ult} is ultimate tensile strength, R_i is internal radius and t is thickness of cylinder.

Moreover, considering the principal stresses, namely hoop stress $\sigma_x = pR_i/t$ and meridional stress $\sigma_y = pR_i/2t$ under unit pressure, it is proposed to take von-mises stress as resultant stress which could be equated to a stress level for failure.,

$$p\sqrt{(\sigma_x^2 + \sigma_y^2 - \sigma_x\sigma_y)} = \sigma_{ys}\left(2 - \frac{\sigma_{ys}}{\sigma_{ult}}\right) \quad (3)$$

Where, the RHS is an empirically proposed stress level lying in between yield and ultimate interpolated with the ratio of yield stress to ultimate stress. Here, σ_{ys} is the yield strength and σ_{ult} is the ultimate tensile strength.

Finite element analysis has an additional advantage that it can be used for both thin and thick cylinders with the same procedure. In this work, an eight-node axisymmetric element type Plane 183 of Ansys software is used. The model is very simple which takes very small memory and computation time. The model is shown in Figure 1(a). After generating the geometric model, meshing is carried out. Mesh density convergence has been studied. Material properties E and ν are specified and stress-strain data is supplied. In order to generate stress-strain data for the analysis, a constitutive material model that gives the stress as an explicit function of strain is used. It is known as inverse of Ramberg- Osgood equation (Liu et al. 2014).

$$\sigma = E\varepsilon\left\{1 + \left(\frac{\varepsilon}{\varepsilon_0}\right)^{n_0}\right\}^{\frac{-1}{n_0}} \quad (4)$$

Where, $\varepsilon_0 = \sigma_{ult}/E$, n_0 is the parameter defining the shape of the non-linear stress-strain relationship. The finite element analysis takes geometric as well as material non-linearities into account. To the finite element, boundary conditions of u_y at bottom edge, an internal pressure p at the inner edge and corresponding $\sigma_y = pR_i/2t$ at the top edge. In the

analysis, the prescribed value of p corresponds to a time unit of 1. For the required precision, the number of sub-steps is specified. The analysis will run to a fraction of 1 which corresponds to a lesser number of sub-steps and will terminate with an indication of rigid body motion. Then the burst pressure would be the time fraction multiplied by the prescribed value of p . Moreover, post-processing would reveal additional details with regard to stress levels and displacements which also would confirm the failure phenomenon. But it is to be noted that the results of stress, strain, etc., will be available in the post processor only up to the sub-step crossed just before termination of the program.

3. Analysis on metal-lined composite pressure vessels

Finite element analysis of composite pressure vessel is carried out with the use of shell elements in a partially revolved surface model. The element type used is shell 281. Isotropic material properties E , E_t and σ_{ult} are the inputs for the metallic liner. Here E_t is tangential modulus, the second slope of the bi-linear material curve. Orthotropic material properties Young's moduli E_1 , $E_2 = E_3$, shear moduli $G_{12} = G_{31}$, G_{23} , and Poisson's ratios $\nu_{12} = \nu_{31}$ and ν_{23} are supplied for the polymer composite material. In general, mechanical properties of composite materials can be determined based on the volume fraction using micromechanics rules such as rule of mixtures, Chamis equations and Halpin-Tsai equations (Rafiee and Amini 2015). The mechanical properties are very much sensitive to the volume fraction and even a small variation of about 10% reflects with 22% variation in the burst pressure (Rafiee and Amini 2015). Hence in cases where manufacturing variability is present, such variations can be treated with stochastic analysis instead of deterministic analysis (Rafiee and Torabi 2018, Rafiee et al. 2015). It is noteworthy that such analysis would require input data in terms of mean, standard deviation and the type of the statistical distribution such as Normal, Lognormal, Weibull etc. Rafiee and Torabi (2018) and Rafiee et

al. (2015) have carried out progressive failure analysis in stochastic analysis mode. The analysis generates number of sample data from the prescribed mean, standard deviation and the type of distribution of the input variables using Monte-Carlo technique. However, the present analysis is deterministic and the composite properties used have been taken from published literature Liu et al. (2014).

In the definition of shell particulars, ply thickness and orientation are specified for all layers including the liner. In order to model the composite cylinder, a straight line representing the generator for the curved surface is created at the specific mean radius with reference to an axis. To represent the axis of revolution, two points are created along the y-axis. The generating line is swept through 90° . The curved surface is meshed with sufficiently small size elements. Final mesh size is arrived at by convergence study. The bottom edge of the surface model is specified with u_y constraint, two vertical edges are specified with symmetric boundary conditions, the internal surface is applied with a pressure of 1 MPa, the top edge is imposed with meridional stress $pR_m/2t$ in which $p = 1$ MPa and $t = 1$. The analysis is always with an internal pressure of 1 MPa. Actual thickness is taken care of by shell definition of ply details. In Figure 1(b) the finite element model is shown. Large deformation option is invoked. After running the analysis, layer -wise stresses are noted. These stresses are then transformed into the material coordinate system of individual plies. Comparing these stresses to relevant strength values, pressure values are obtained. Out of the three values of p calculated for all the layers, the most minimum value will indicate first ply failure pressure (p_1). It also indicates the failed layer and mode of failure whether fibre or matrix or shear. The stresses computed at this stage would be multiplied with pressure 0 to p_1 in order to have actual stress history on loading. Now, for the progressive analysis, the failed layer is to be degraded.

Rafiee et al. (2018) have dealt with a four-step procedure in progressive analysis including modelling, evaluation of stress, evaluation of failure pressure and material degradation. They employed both CDM approach as well as ply discount method in which results were accurate with first approach and underestimated with the latter. CDM approach involves the use of a damage evolution model where as ply discount method is associated with degradation of failed layers for which they have prescribed guidelines. Present approach is very much similar to the ply discount method described by them. But in order to reduce the inaccuracies at the same time solving the problem of solution convergence, certain rules are laid down after repeated trials. Accordingly, the analysis is carried out here. Important one is that the applied pressure is always 1 MPa and stresses are extrapolated based on the strength parameters. If the failure noticed is in the matrix, it is understood that the layer cannot contribute to stiffness in transverse and shear directions. In order to degrade the stiffness values to near-zero level, if a multiplication factor of 10^{-6} , is used in those directions, the convergence of the solution is not achieved especially when few layers remain un-failed. Multiplication factor of 10^{-1} is highly insufficient and produces inaccurate results. After repeated trials of analysis, the multiplication factor of 10^{-3} is used for the failed orientation. Moreover, in the case of matrix failure, it is not reasonable to leave the fibre orientation as it is. After the matrix failure, it is highly improbable that fibre continues to contribute to same stiffness in its direction. On trying this possibility, it has been found that other un-failed layers were under-stressed which lead to inaccurate solutions. Hence it is practiced with a multiplication factor of 10^{-1} for stiffness degradation of fibre direction and it is taken that the layer in full is failed. Similarly, in the case of fibre failure, multiplication factors are alternatively used, but it is 10^{-3} for shear orientation. The maximum pressure recorded in the analysis will be the bursting pressure. Corresponding calculated stress values are used to get the actual stress history in the range $p_1 - p_2$, $p_2 - p_3$, and so on till the bursting pressure. The

present analysis being deterministic, for a particular cylinder, one value of first ply failure pressure and one value of burst pressure will be obtained. If stochastic analysis is carried out with random variables of property values as chosen by Monte-Carlo technique (Rafiee and Torabi 2018, Rafiee et al. 2015), as many numbers of first ply failure pressure and burst pressure are obtained as number of iterations. From these values, mean, standard deviation and type of distribution will be evaluated and presented. This statistical output is the response of manufacturing inconsistencies which affect the properties of composites (Rafiee and Torabi 2018).

4. Results and discussion

18% Ni maraging steels are the most preferred metallic materials for aerospace utilities. Its prime advantage lies in the characteristics of malleability, stable properties at higher temperatures, and slow softening. It has a high strength to weight ratio among metals. It has an additional advantage of very minimum hardening and produces very few cracks during welding (Christopher et al. 2004). Wei (1965) carried out burst-tests on rocket motor cases made of few materials including 18% Ni maraging steel. Few failure data are chosen from his paper for demonstrating the present work. The cylinder dimensions and material properties are presented in Table 1.

Simple equations (2) and (3) are substituted with the data for the three cylinders to obtain burst pressure as per Svensson's analysis and present analysis. Both are giving very close results with the experimental values as presented in Table 2. In the FEA, the pressure applied are 12, 12 and 60 MPa respectively on three cylinders all corresponding to time unit 1. The sub-steps specified are 24, 24 and 60 respectively. Ansys gave the failure time as 0.91667, 0.708333 and 0.983333 respectively at the instant of termination with reported rigid body motion. When these factors are multiplied with the pressure applied, corresponding

failure pressures are obtained. These are presented in table 2. Ansys displays a further message that the rigid body motion could occur when net section yielding occurs, resulting in large displacements for small increments of load. This can be confirmed from Table 3 in which there is sudden increase in displacement for the same pressure near 59 MPa. This conveys a loss of stiffness. Also, an understanding is derived from the work of Svensson (1958) that just before failure, the plastic zone spreads to the outer surface. Hence Von-Mises stress vs. applied internal pressure is plotted till failure. It is observed that the inner surface stress advances to ultimate tensile strength level faster and subsequently same thing happens to the outer surface also. When both the surfaces are stressed to the ultimate strength, failure of pressure vessel occurs. This phenomenon is shown clearly in Figure 2.

Hydrogen storage vessels of different capacities for aerospace applications have been burst tested and analysed by Liu et al. (2014). Three cylinders namely A, B, and C have dimensions and ply details as detailed in Table 4. The properties of liner material 6061-T6 Aluminium alloy is presented in Table 5. Properties of T 700 carbon/epoxy composite are presented in Table 6. As an attempt, vessel B was analysed in which the liner material was modelled with continuous stress–strain curve using equation (4), instead of a bi-linear curve. The material constants are $\epsilon_0 = 0.004629$, $n_0 = 1.5$. The first ply failure was in layer 5 at 43.71 MPa. The order of failure was 5-3-4-7-8-10-9-1-2-6-11 with layer 2 recording the maximum pressure of 127.41 MPa. The solution running time was very long due to non-linearity with regard to both geometry and material and hence the procedure is not convenient for repetition.

Subsequently, all the three vessels are analysed using the procedure outlined in section 3. The details of the failure are presented for cylinder B only by post-processing the stress history. In this cylinder, the first ply failure took place in the layer 5 at the same pressure as of previous exercise above. Subsequently except the three hoop layers (2, 6 and

11), all other layers including metallic liner failed within about 50 MPa in the order 10-3-9-8-7-4-1. All of the above layers failed in matrix. It may be noted that all these layers having ply orientations 38° , 12.3° , 32° , 27° , 22° and 15.4° (refer Table 4) which are close to the meridional direction of the cylinder. Hence, they are liable to matrix failure by hoop stress. Layer 1 is metallic liner. At a pressure of 122.9 MPa, failure of layer 2 was revealed along fibre direction and layers 6 and 11 recorded lower stresses. However, on further loading, layers 6 and 11 failed one after the other under lower pressures in fibre direction. Therefore, the maximum recorded value of pressure is taken as the burst pressure. This is clearly shown in Figure 3. Figure 4 shows the order of failure and the failed pressure levels. Table 7 shows radial displacement in vessel B. It may be noted that a sudden fall of pressure with a large displacement indicates burst. Table 8 shows a comparison of first ply failure pressure and burst pressure predictions by the present analysis with the test results (Liu et al. 2014). Liu et al. (2014) have not presented the exact first ply failure pressure by test but mentioned that the composite layers started failing under about 40 MPa. The high burst pressure levels signify the optimum thickness and winding angle of composite layers, especially the suitably placed hoop layers.

5. Conclusions

An empirical relation for the prediction of burst-pressure of metallic cylinder is proposed in this paper. Burst pressure estimates of 18% Ni Maraging steel rocket motor cases were within $\pm 5.8\%$ of test results. The finite element analysis-based procedure described in the paper visualizes the failure phenomenon in terms of displacement as well as effective stress. The failure predictions on the same materials are within $\pm 10\%$ of test results. Two types of material modelling have been tried for the metal liner in the burst pressure prediction of 6061-T6 aluminium lined T700 carbon/epoxy composite pressure vessels. Though

continuous form of material curve gives more realistic results, high processing time is at disadvantage for repeated analyses. Bi-linear modelling also gives reasonably good results and it is faster in solving. The extent of degradation demonstrated in this analysis has been found to give consistent results. Burst pressure predictions of the three vessels were within +8.2 %. The stress history and displacement history give better comprehension with regard to the progressive failure.

Reference

- Bai, H., Yang, B., Hui, H., Yang, Y., Yu, Q., Zhou, Z., Xian, P. 2019. Experimental and numerical investigation of the strain response of the filament wound pressure vessels subjected to pressurization test. *Polymer Composites*. **40**(11): 4427–4441. [doi:10.1002/pc.25304](https://doi.org/10.1002/pc.25304).
- Beena, A.P., Sundaresan, M.K., NageswaraRao, B. 1995. Destructive tests of 15CDV6 steel rocket motor cases and their application to lightweight design. *International Journal of Pressure Vessels and Piping* . **62**(3): 313-320. [doi:10.1016/0308-0161\(94\)00026-F](https://doi.org/10.1016/0308-0161(94)00026-F).
- Chang, R.R. 2000. Experimental and theoretical analyses of first-ply failure of laminated composite pressure vessels, *Compos Struct*. **49**(2): 237–243. [doi:10.1016/S0263-8223\(99\)00133-6](https://doi.org/10.1016/S0263-8223(99)00133-6).
- Christopher, T., Sankarnarayanan, K., Rao, B.N. 2004. Fracture behaviour of maraging steel tensile specimens and pressurized cylindrical vessels. *Fatigue and Fracture of Engineering Materials and Structures*. **27**(3): 177–186. [doi:10.1111/j.1460-2695.2004.00673.x](https://doi.org/10.1111/j.1460-2695.2004.00673.x).
- Christopher, T., Sarma, B.S.V.R., Potti, P.K.G., Rao, B.N. 2002. A comparative study on failure pressure estimations of unflawed cylindrical vessels. *International Journal of Pressure Vessels and Piping*. **79**(1): 53–66. [doi:10.1016/S0308-0161\(01\)00126-0](https://doi.org/10.1016/S0308-0161(01)00126-0).
- Hu, J., Sundararaman, S., Menta, V.G.K., Chandrashekhara, K., Chernicoff, W. 2009. Failure pressure prediction of composite cylinders for hydrogen storage using thermo-mechanical analysis and neural network. *Advanced Composite Materials*. **18**(3): 233–249. [doi:10.1163/156855109X428790](https://doi.org/10.1163/156855109X428790).
- Kadam, M., Gopalsamy, B., Bujurke, A.A., Joshi, K.M. 2018. Estimation of static burst pressure in unflawed high pressure cylinders using nonlinear FEA. *Thin-Walled Structures*. **126**: 79–84. [doi:10.1016/j.tws.2017.05.022](https://doi.org/10.1016/j.tws.2017.05.022).

- Kalaycioglu, B., Dirikolu, M.H. 2010. Investigation of the design of a metal-lined fully wrapped composite vessel under high internal pressure. *High Pressure Research: An International Journal*. **30**(3): 428–437. [doi:10.1080/08957959.2010.504420](https://doi.org/10.1080/08957959.2010.504420).
- Kam, T.Y., Liu, Y.W., Lee, F.T. 1997. First-ply failure strength of laminated composite pressure vessels. *Composite Structures*. **38**: 65–70. [doi:10.1016/S0263-8223\(97\)00042-1](https://doi.org/10.1016/S0263-8223(97)00042-1).
- Kaw, K. 2015. *Mechanics of composite materials*. 2nd ed., Taylor & Francis. Boca Raton: CRC Press.
- Liu, P.F., Xing, L.J., Zheng, J.Y. 2014. Failure analysis of carbon fiber/epoxy composite cylindrical laminates using explicit finite element method. *Composites Part B: Engineering*. **56**: 54–61. [doi:10.1016/j.compositesb.2013.08.017](https://doi.org/10.1016/j.compositesb.2013.08.017).
- Margetson, J. 1978. Burst pressure prediction of rocket motors. In: *Proceedings of the fourteenth Joint Propulsion Conference, AIAA/SAE, Las Vegas, NV USA*. AIAA paper no. 78-1567.
- Martins, L.A.L., Bastian, F.L., Netto, T.A. 2014. Reviewing some design issues for filament wound composite tubes. *Materials and Design*. **55**: 242–249. [doi:10.1016/j.matdes.2013.09.059](https://doi.org/10.1016/j.matdes.2013.09.059).
- Rafiee, R., Amini, A. 2015. Modeling and experimental evaluation of functional failure pressures in glass fiber reinforced polyester pipes. *Computational Materials Science*. **96**(B): 579-588. [doi:10.1016/j.commatsci.2014.03.036](https://doi.org/10.1016/j.commatsci.2014.03.036).
- Rafiee, R., Elasmı, F. 2017. Theoretical modeling of fatigue phenomenon in composite pipes. *Composite Structures*. **161**: 256-263. [doi:10.1016/j.compstruct.2020.112646](https://doi.org/10.1016/j.compstruct.2020.112646).
- Rafiee, R., Reshadi, F., Eidi, S. 2015. Stochastic analysis of functional failure pressures in glass fiber reinforced polyester pipes. *Materials & Design* **67**: 422-427. [doi:10.1016/j.matdes.2014.12.003](https://doi.org/10.1016/j.matdes.2014.12.003).
- Rafiee, R., Torabi, M.A. 2018. Stochastic prediction of burst pressure in composite pressure vessels. *Composite Structures*. **185**: 573-583. [doi:10.1016/j.compstruct.2017.11.068](https://doi.org/10.1016/j.compstruct.2017.11.068).
- Rafiee, R., Torabi, M.A., Maleki, S. 2018. Investigating structural failure of a filament-wound composite tube subjected to internal pressure: Experimental and theoretical evaluation. *Polymer Testing*. **67**: 322-330. [doi:10.1016/j.polymertesting.2018.03.020](https://doi.org/10.1016/j.polymertesting.2018.03.020).
- Sleight, D.W. 1999. *Progressive Failure Analysis Methodology for Laminated Composite Structures*, NASA/TP-1999-209107.

Sorrentino, L., Tersigni, L. 2015. Performance index optimization of pressure vessels manufactured by filament winding technology. *Advanced Composite Materials*. **24**(3): 269–285. [doi:10.1080/09243046.2014.887429](https://doi.org/10.1080/09243046.2014.887429).

Svensson, N.L. 1958. Bursting pressure of cylindrical and spherical vessels. *Trans ASME J Appl Mech*. **80**(3): 89-96.

Wei, B.C.F. 1965. Destructive tests of full-size rocket motor cases and their application to lightweight design. *Journal of Spacecraft and Rockets*. **2**: 363–368. [doi:10.2514/6.1964-445](https://doi.org/10.2514/6.1964-445).

Wolford, G.F., Hyer, M.W. 2005. Failure initiation and progression in internally-pressurized elliptical composite cylinders. *Mechanics of Advanced Materials and Structures*. **12**: 437–455. [doi:10.1080/15376490500259269](https://doi.org/10.1080/15376490500259269).

Wu, Q.G., Chen, X.D., Fan, Z.C., Nie, D.F. 2015. Stress and Damage Analyses of Composite Overwrapped Pressure Vessel. *Procedia Engineering*. **130**: 32–40. [doi:10.1016/j.proeng.2015.12.171](https://doi.org/10.1016/j.proeng.2015.12.171).

Xu, P., Zheng, J.Y., Liu, P.F. 2009. Finite element analysis of burst pressure of composite hydrogen storage vessels. *Materials and Design*. **30**(7): 2295–2301. [doi:10.1016/j.matdes.2009.03.006](https://doi.org/10.1016/j.matdes.2009.03.006).

Table 1 Dimensions and material properties of 18% Ni maraging steel**rocket motor cases (Wei 1965) ($E = 2 \times 10^5$ MPa, $\nu = 0.3$, $n=0.05$)**

σ_{ys} (MPa)	σ_{ult} (MPa)	Inner Diameter	Thickness (mm)	n_0	σ_0 (MPa)
2006	2062	1663.7	3.7	3	0.01031
1937	2013	1016.0	1.8	3	0.01007
1937	2006	157.2	2.0	3	0.01003

Table 2 Comparison of burst pressure predictions of rocket motor cases by various approaches

Cylinder #	Test (Wei 1965)	Burst pressure, MPa		
		Svensson's formula (2)	Present Analysis (3)	Present FEA
1	10	10.30	10.58	11.000
2	8	8.01	8.22	8.499
3	60	57.34	58.87	58.999

Table 3 Radial displacement (u_r) vs Internal pressure (p_i) in cylinder 3 in the present work

p_i , MPa	10	20	30	40	50	58
u_r , mm	0.14	0.27	0.42	0.62	0.96	3.57

Table 4 6061T-6 Aluminium lined T700/epoxy Cylinder dimensions and shell details (Liu et al. 2014)

	Cylinder A, $R_i=44$ mm		Cylinder B, $R_i=91.5$ mm		Cylinder C, $R_i=98.5$ mm	
Layer #	Layer angle, (°)	Thickness, mm	Layer angle, (°)	Thickness, mm	Layer angle, (°)	Thickness, mm
1.	liner	1.8	liner	5	liner	5
2.	90	0.42	90	2.1	90	1.8
3.	90	0.42	12.3	0.87	12.3	0.73
4.	18.6	0.42	15.4	0.87	15.4	0.73
5.	-18.6	0.42	18.6	0.87	18.6	0.73
6.	90	0.42	90	2.1	90	1.8
7.	90	0.42	22	0.87	22	0.73
8.	28.9	0.42	27	0.87	27	0.73
9.	-28.9	0.42	32	0.87	32	0.73
10.	90	0.42	38	0.6	38	0.5
11.	90	0.42	90	0.54	90	0.45

Table 5 Material properties of 6061-T6 Aluminum liner (Liu et al. 2014)

E, MPa	ν	E_t , MPa	σ_{ys} , MPa	σ_{ult} , MPa
70000	0.33	600	246	324

Table 6 Material properties of T700 carbon/epoxy polymer composite (Liu et al. 2014)

Elastic properties		Strength properties	
E_1 , MPa	154100	X_T , MPa	2500
$E_2=E_3$, MPa	10300	X_C , MPa	1250
$G_{12}=G_{31}$, MPa	7090	Y_T , MPa	60
G_{23} , MPa	3790	Y_C , MPa	186
$\nu_{12}=\nu_{13}$	0.28	S , MPa	85
ν_{23}	0.49	T , MPa	85

Table 7 Radial displacement (u_r) vs Internal pressure (p_i) in vessel B by present analysis

p_i , MPa	20	40	60	80	100	122.9	97.54	29.93
u_r , mm	0.11	0.21	0.85	1.14	1.42	1.75	2.30	3.80

Table 8 Comparison of first ply failure and burst pressure results of metal-lined polymer composite pressure vessels

Cylinder id	First ply failure pressure-Test (Liu et al. 2014) MPa	First ply failure pressure-Present, MPa	Burst pressure-Test (Liu et al. 2014) MPa	Burst pressure-Present, MPa
A	-	8.97	106.00	102.82
B	≈ 40	43.71	125.00	122.90
C	≈ 40	36.61	99.88	91.68

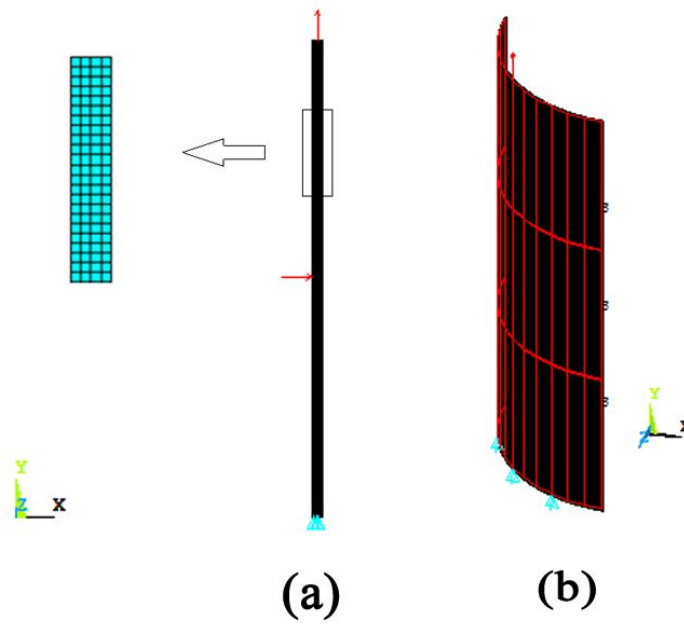


Figure 1 Finite element model of (a) metallic and (b) metal-lined polymer composite pressure vessels

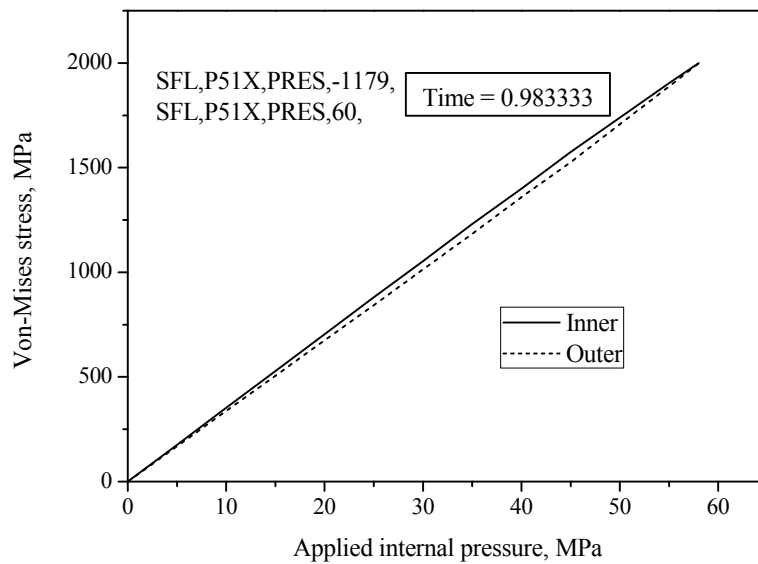


Figure 2 Von-Mises stress plot for cylinder 3

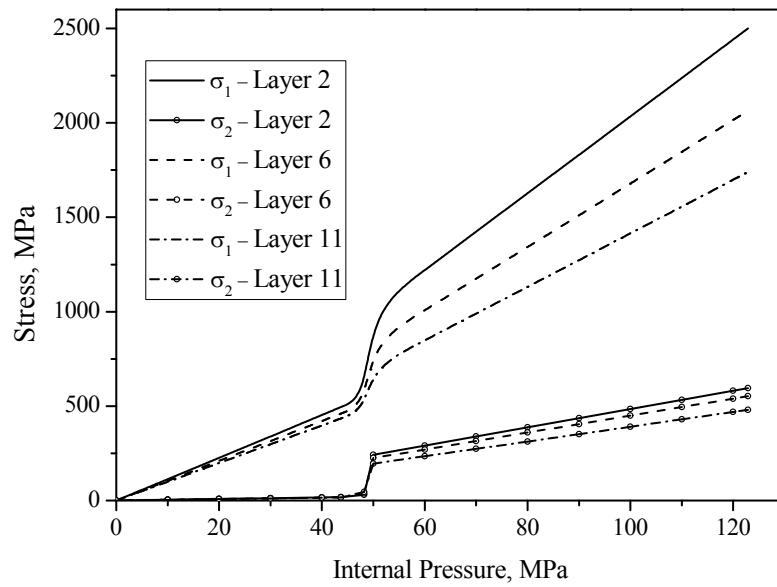


Figure 3 Stress history for finally failed layers of metal-lined composite pressure vessel B

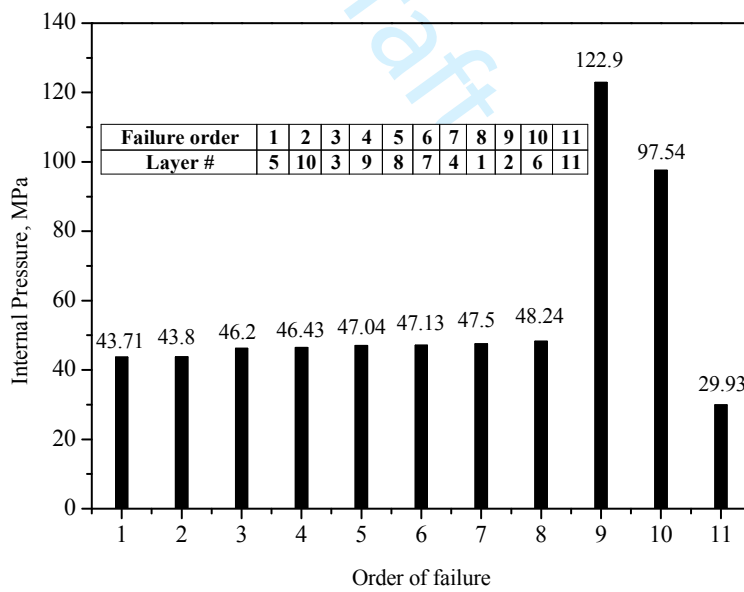


Figure 4 Order of failed plies in metal-lined composite pressure vessel B